

Review

Not peer-reviewed version

Unveiling the Potential of Cryogenic Post-Combustion Carbon Capture: From Fundamentals to Innovative Processes

[Mauro Luberti](#) , [Erika Ballini](#) , [Mauro Capocelli](#) *

Posted Date: 8 May 2024

doi: [10.20944/preprints202405.0429.v1](https://doi.org/10.20944/preprints202405.0429.v1)

Keywords: CO₂ sequestration; cryogenics; thermodynamics; desublimation; process configuration; energy consumption



Preprints.org is a free multidiscipline platform providing preprint service that is dedicated to making early versions of research outputs permanently available and citable. Preprints posted at Preprints.org appear in Web of Science, Crossref, Google Scholar, Scilit, Europe PMC.

Copyright: This is an open access article distributed under the Creative Commons Attribution License which permits unrestricted use, distribution, and reproduction in any medium, provided the original work is properly cited.

Disclaimer/Publisher's Note: The statements, opinions, and data contained in all publications are solely those of the individual author(s) and contributor(s) and not of MDPI and/or the editor(s). MDPI and/or the editor(s) disclaim responsibility for any injury to people or property resulting from any ideas, methods, instructions, or products referred to in the content.

Review

Unveiling the Potential of Cryogenic Post-Combustion Carbon Capture: From Fundamentals to Innovative Processes

Mauro Luberti ¹, Erika Ballini ² and Mauro Capocelli ^{2,*}

¹ Department of Chemical Engineering, School of Engineering, The University of Manchester, Oxford Road, Manchester M13 9PL, UK; mauro.luberti@manchester.ac.uk

² Research Unit of Process Engineering, Department of Science & Technology for Sustainable Development & One Health, University Campus Bio-Medico di Roma, Via Alvaro del Portillo, 21, 00128 Rome, Italy

* Correspondence: m.capocelli@unicampus.it

Abstract: Climate change necessitates urgent actions to mitigate carbon dioxide (CO₂) emissions from fossil fuel-based energy generation. Among various strategies, the deployment of carbon capture and storage (CCS) solutions are critical for reducing emissions from point sources such as power plants and heavy industries. In this context, cryogenic carbon capture (CCC) via desublimation has emerged as a promising technology. While CCC offers high separation efficiency, minimal downstream compression work, and integration potential with existing industrial processes, challenges such as low operating temperatures and equipment costs persist. Ongoing research aims to address these hurdles in order to optimize the desublimation processes for widespread implementation. This review consolidates diverse literature works, providing insights into the strengths and limitations of CCC technology, including the latest pilot plant scale demonstrations. The transformative potential of CCC is first assessed on a theoretical basis, such as thermodynamic aspects and mass transfer phenomena. Then, recent advancements in the proposed process configurations are critically assessed and compared through key performance indicators. Furthermore, future research directions for this technology are clearly highlighted.

Keywords: CO₂ sequestration; cryogenics; thermodynamics; desublimation; process configuration; energy consumption

1. Introduction

It is now widely recognized that climate change, standing as the most pressing challenge of our time, is driven primarily by anthropogenic activities. Among the unequivocal evidence there are rising global temperatures, melting polar ice caps, ocean acidification phenomena, and increasingly erratic weather patterns [1]. In the pursuit of mitigating these impacts, the scientific community has tirelessly explored various strategies to reduce carbon dioxide (CO₂) emissions such as [1,2]:

- Improvement of fossil fuel-based energy efficiency;
- Enhancement of nuclear and renewable energy as well as increasing use of biofuel-based energy;
- Development of environmental engineering works such as afforestation and reforestation.

On the other hand, during this period of ecological transition and contextual energy crisis, the belief of making our current economies independent from fossil fuels seems a utopia as the above mitigation strategies alone may fall short in achieving the necessary emission reductions [3,4]. Carbon capture and storage (CCS) would serve as a critical bridge, allowing industries with substantial point-source CO₂ emissions, such as power generation and heavy manufacturing, to significantly curtail their carbon footprint.

After the capture process, CO₂ is usually compressed and transported via pipelines to the storage or utilization facilities. In geographical regions without extensive pipeline infrastructure, CO₂ could be transported in the liquid phase via ships. CO₂ could then be injected and stored underground in

geological formations such as depleted oil and gas wells, saline aquifers, and deep coal seams. CO₂ could also react with certain minerals to form stable carbonates, providing a long-term storage solution. Moreover, CO₂ utilization (CCU) involves converting the captured CO₂ into valuable products, such as bulk chemicals, plastics, and synthetic fuels. This strategy, although energy and/or hydrogen intensive, offers advantages in offsetting the cost of carbon capture by creating revenue streams [2–5].

The rising emphasis on achieving a net-zero society by mid-century, as articulated in international agreements and embraced by nations and corporations alike, has propelled CCS into the forefront of climate change solutions. Policies and financial incentives aimed at fostering CCS deployment further underscore its integral role in achieving the decarbonization goals [3–5]. The key role of CCUS in reducing the CO₂ emissions can be justified by a number of reasons:

- For decades to come, electricity generation will still rely on fossil fuels (due to the estimated lifetime of recently built or planned coal- and NG-based power plants) with estimated CO₂ emissions of 25 Gt between 2020 and 2070 [5–7];
- CCUS can be easily integrated into existing energy and utility systems, without invasive or complex retrofits;
- CCUS is currently the only viable option for decarbonizing emission-intensive industries (iron and steel, cement, chemicals and petrochemicals) where the majority of CO₂ emissions arise from the combustion of fossil fuels to generate high temperature heat duties [6,7];
- CCUS can be implemented for the production of low-carbon hydrogen (blue hydrogen): currently, around 76% of hydrogen (corresponding to 75 Mt y⁻¹) is produced worldwide from natural gas, generating overall CO₂ emissions exceeding 800 Mt y⁻¹ [8]; green hydrogen produced by electrolysis is still expensive having a cost of 2.3–6.9 \$ t_{H2}⁻¹ versus 1.4–2.4 \$ t_{H2}⁻¹ from steam methane reforming (SMR) coupled with CCS [8,9];
- CCUS has been regarded as a pivotal technology for allowing carbon negative emissions if applied to plants processing biofuels and wastes (BECCS) or directly to atmospheric air (DAC) [3,4,10].

So far, diverse CCS technologies have been proposed, however the quest for an efficient, scalable and low-cost solution remains ongoing. Although the deployment of CCS projects has seen a notable progress, the amount of CO₂ captured and sequestered is overall relatively modest. Up to now, only a few Mt of CO₂ have been captured globally, with various projects demonstrating the feasibility of CCS in different industrial settings. However, meeting the scale required for a meaningful climate impact would require a remarkable upscaling of CCS units. The International Energy Agency (IEA) has anticipated a substantial increase in the capture and storage of CO₂, reaching Gt-scale levels by mid-century [5,6]. According to the IEA report, the Sustainable Development Scenario will meet the energy-related goals by fully eliminating CO₂ emissions by 2070 [5,6]. Butnar et al. [11] examined different scenarios for the European decarbonization, demonstrating that Europe needs a large-scale CCS industry to achieve the future goals. In the 1.5°C scenario, the average CO₂ captured by CCS would be in the range of 230–430 Mt_{CO2} y⁻¹ by 2030 and 930–1200 Mt_{CO2} y⁻¹ by 2050. Koelbl et al. [12] compared 18 integrated assessment models showing that, although carbon capture rates will fluctuate in a wide range in the period 2020–2100, no model predicts less than 600 Gt_{CO2} of cumulated captured emissions.

The selection of a specific capture technology depends on several factors such as the CO₂ concentration of in the gas stream, the target CO₂ purity and CO₂ recovery, the allowed energy requirements and additional constraints based on the specific industrial process. Three main strategies have been presented as follows. In post-combustion capture, CO₂ is captured from the flue gases arising from the combustion of fossil fuels [13]. Pre-combustion capture involves capturing CO₂ from H₂-rich gas mixtures generated by the gasification of fossil fuels prior to the combustion [14]. Oxy-fuel combustion involves burning fossil fuels in an atmosphere enriched with oxygen rather than air [14]. This results in a flue gas stream predominantly composed of CO₂ and water vapor, making it easier to separate CO₂. A further strategy is offered by chemical looping combustion, which separates CO₂ by using metal oxides as oxygen carriers being circulating between two reactors [15].

Among the main carbon capture technologies, amine-based absorption has gained prominence for its efficacy in capturing CO₂ from industrial flue gases. Examples of amine-based solvents are monoethanolamine (MEA), diethanolamine (DEA), and proprietary amines. After the absorption process, the CO₂-rich solvent is regenerated by providing heat to release the captured CO₂ [16]. Alternative solvents such as ionic liquids have also been proposed as they offer some advantages with respect to amines, including low volatility, low regeneration temperatures and potential for tunability [17]. In pressure swing adsorption (PSA) processes, nanoporous adsorbents, such as zeolites and metal organic frameworks, selectively adsorb CO₂ at high pressure. The adsorbent is then regenerated at low pressures, sometimes under vacuum, to release the captured CO₂ [18,19]. Temperature swing adsorption (TSA) processes rely on temperature variations to desorb CO₂ from the adsorbent material. Besides, membrane technology based on polymeric, metallic or ceramic materials, use selective permeable membranes to separate CO₂ from other flue gases by exploiting differences in molecular size, shape, or affinity [20].

As the demand for more sustainable and energy-efficient solutions grows, attention has turned to cryogenic carbon capture as a promising technology in this field. Cryogenic separation involves cooling the flue gas stream to very low temperatures, causing CO₂ to condense or desublimate while the other gases remain in the gaseous phase. Cryogenics refers most closely to processes that occur at temperatures below 120 K (-153°C), such as the condensation of nitrogen and oxygen; however, the term is often used to indicate in a generic way low-temperature separations [21]. While the idea of cryogenic separation has been explored for decades, recent advancements and successful pilot projects have reignited interest in its potential as a game-changing carbon capture technology [21,22]. The earliest works on cryogenic flue gas treatment were developed by the Bechtel Power Corporation on cryogenic SO₂ capture from a coal plant [22]. In the last few decades, many patents were filed in relation to CH₄ purification. Holmes and Ryan [23] proposed a conventional cryogenic distillation for the separation of CH₄ from CO₂ with extractive distillation [23] using an entrainment solvent (heavy hydrocarbon such as n-butane) to control the CO₂ freezing. Amongst other technologies, the CryoCell® process was developed by Cool Energy and tested in collaboration with other industrial partners including Shell Global Solutions in order to cryogenically remove CO₂ from natural gas [24].

In the field of post-combustion carbon capture, cryogenic separation is considered energy-intensive but highly effective. The numerous advances in the cryogenic sector have pushed research to also adopt CCS solutions to treat combustion flue gases. However, several works were related to vapor-liquid equilibrium and therefore limited to gas purifications having a high concentration of CO₂ in the feed stream [25,26]. For instance, Berstad et al. [27] analysed low-temperature CO₂ capture processes from IGCC plants by condensation and phase separation, identifying feasible design configurations and determining a specific energy requirement of around 300 kJ kg⁻¹CO₂ with a CO₂ capture recovery of 85%.

More recently, various scientific works have identified the importance of vapor-solid equilibrium to achieve high CO₂ purities and recoveries, even from flue gases at low pressures and low CO₂ concentrations, and have thus laid the foundation for the thermodynamic understanding and engineering principles of cryogenic desublimation. For instance, some research groups have proposed cryogenic packed beds operating in parallel and undergoing different cycle steps [28,29]. Other researchers have developed prototypes and the first pilot plants based on CO₂ desublimation, showcasing the feasibility of implementing cryogenic carbon capture [30]. Overall, according to the literature reviewed in the present work, cryogenic carbon capture (CCC) based on CO₂ desublimation from post-combustion flue gases offers several advantages compared to other technologies as follows:

- The technology features extremely high selectivity, and thus minimizes the competitive capture of other components in the flue gases;
- The separation process is driven by temperature differences and does not rely on solvents, adsorbents or membranes;
- The CO₂ product is generally extracted in the liquid phase, so as to avoid the downstream compression work;

- Scalability potential and wide ranges of applications have been demonstrated. In addition, CCC can be integrated into existing industrial processes with minimal retrofit requirements;
- CCC is characterized by low water consumption and offers a large heat integration potential. This, in turn, minimizes the disposal of wastes and enhances safety and environmental aspects.

While these advantages make CCC an intriguing option, it is also important to acknowledge that several challenges exist, including the need for very low operating temperatures, the high cost of equipment materials, and the overall feasibility of large-scale implementation. Ongoing research and developments are essential to address these challenges and optimize CCC for widespread application. In the last few years various review articles have been published discussing both modelling and experimental aspects of cryogenic desublimation methods for post-combustion carbon capture [21,26,31–33].

Shen et al. [26] focused on the cryogenic capture systems from the perspective of constructing new cryogenic capture system structures, exploring the optimal system parameters, and analyzing the challenges faced. Font-Palma et al. [21] presented a first comprehensive review on the topic. Song et al. [31] systematically discussed several CCC technologies, including standalone process schemes and hybrid schemes coupled with cold sources such as LNG regasification [31]. Asgharian et al. [32] published a review paper on process modeling of CCC, focusing on thermodynamics and energy-related aspects. Aneesh and Sam [33] evaluated additional theoretical aspects of CCC technologies such as mass transfer mechanisms.

All the above works often focussed on a limited research area, either thermodynamic aspects or process configurations. Furthermore, these works often included process schemes that are based on vapor-liquid equilibrium and/or hybrid schemes to purify CH_4 rather than capturing CO_2 . This means that the presented results are heterogeneous and do not represent a systematic classification of the processes based on cryogenic desublimation. In addition, desublimation-based technology is experiencing a rising interest with the first demonstration pilot plants being built and operating, which could confirm the theoretical and modelling aspects investigated in the previous papers.

Based on these considerations, a novel and comprehensive review work on this topic is necessary. This paper delves into the evolution of cryogenic carbon capture by desublimation, emphasizing both strengths and limitations of the latest process schemes. It meticulously explores the engineering principles behind desublimation, ranging from thermodynamics to mass transfer phenomena. By critically evaluating the achievements of pilot plants and commercial solutions, we aim to elucidate the transformative potential of cryogenic carbon capture, shedding light on recent breakthroughs and real-world applications. This will be achieved by discussing the main process schemes and comparing the key performance indicators of the proposed technologies.

2. Fundamentals of Cryogenic Desublimation

To predict the phase equilibria involved in cryogenic desublimation processes, cubic equations of state (EoS) including Soave–Redlich–Kwong (SRK), Peng–Robinson (PR) and Patel–Teja (PT) can be used coupled with a relatively small amount of experimental data to determine their mixing rules parameters [34]. Several works studied theoretically and experimentally CO_2 desublimation in the oil and gas industry. De Guido et al. [35] demonstrated the reliability of their thermodynamic modelling in representing solid-liquid-vapor equilibrium (SLVE) with a focus on obtaining CO_2 solubility predictions in hydrocarbon-rich mixtures (notably for natural gas purification). The same authors also described the solid-vapor equilibrium (SVE) for $\text{CO}_2\text{-CH}_4$ and $\text{CO}_2\text{-CH}_4\text{-N}_2$ mixtures applying both selected cubic EoS and the Gibbs energy minimization method [36]. A parallel field of studies was also related to the prediction of the Joule–Thomson effect, where Wang et al. [37] developed and validated an improved 25-parameter model. Below is reported the most commonly used set of equations to describe SVE of CO_2 in a flue gas mixture as well as to predict CO_2 dew and freezing points. In particular, Equation (1) represents the isofugacity condition for the SVE, while the PR EoS shown in Equation (2) is used to calculate the fugacity coefficients of CO_2 in both solid and vapor phases. The sublimation vapor pressure of CO_2 can be determined by Equation (3), as tested by Jensen et al. [30].

$$\phi_{CO_2}^S \cdot P_{CO_2}^S \cdot e^{\frac{v_{CO_2}^S \cdot (P - P_{CO_2}^S)}{RT}} = y_{CO_2} \cdot \phi_{CO_2}^V \cdot P \quad (1)$$

$$P = \frac{R \cdot T}{v - b} - \frac{a(T)}{v \cdot (v + b) + b \cdot (v - b)} \quad (2)$$

$$P_{CO_2}^S = \exp \left[57.52 + \frac{-3992.84}{T} - 4.9003 \cdot \ln(T) + 2.415 \cdot 10^{-15} \cdot T^6 + \frac{8125.6}{T^2} \right] \quad (3)$$

In the above equations y_{CO_2} , $\phi_{CO_2}^V$, P , $P_{CO_2}^S$, $\phi_{CO_2}^S$ and $v_{CO_2}^S$ represent the mole fraction of CO₂ in the vapor phase, the fugacity coefficient of CO₂ in the vapor phase, the total pressure, the sublimation vapor pressure of CO₂, the fugacity coefficient of CO₂ at the saturated solid pressure and the molar volume of solid CO₂, respectively. It should be noted that in Equation (1) the solid phase is represented by pure CO₂. Several modifications of the above equations are reported in the literature, especially for the binary interaction parameters of the cubic EoS [30,38,39]. In the works of both Jensen et al. [30] and Pellegrini et al. [38], SVE calculations have been implemented by minimizing the Gibbs energy of the system. Most theoretical data have also been validated through dedicated experimental campaigns [30,38].

In this work similar results based on SVE were achieved using Aspen Plus V10.0 software. To obtain these data the RGibbs reactor was selected. The CO₂ solid phase is formed as a result of a chemical equilibrium reaction from the gas phase. The results were obtained for binary systems of CO₂ and N₂ considering two CO₂ concentrations in the feed: 5 mol% as representative for natural gas-fired power plant flue gases and 15 mol% as representative for coal-fired power plant flue gases.

Figure 1a shows the CO₂ recovery in the solid phase against the flue gas temperature according to the SVE model at three different pressure levels and two inlet CO₂ concentrations. Figure 1b shows the flue gas temperature required to obtain a certain CO₂ recovery in the solid phase at a given pressure starting with a flue gas having a CO₂ composition of 15%. In Figure 1b simulation results are compared against the calculations carried out by Pellegrini et al. [38] and Baxter et al. [40]. In case of low CO₂ concentrations (5%) in the feed, high CO₂ recoveries are achievable only by operating at temperatures below 150 K or considering flue gases at higher pressures. However, these temperature levels could be raised to around 170 K if the flue gases contain 15% of CO₂ at relatively low pressures.

Overall, it is possible to obtain a minimum work of separation in the order of 1 MJ kg_{CO₂}⁻¹ at these temperatures and for inlet CO₂ concentrations of around 15%. Yurata et al. [41] carried out process simulations involving CO₂-H₂ mixtures demonstrating the thermodynamic superiority of desublimation processes against other unit operations. Energy consumption values of 1–2 MJ kg_{CO₂}⁻¹ represent an enormous advantage compared to the state of the art of technology, especially considering that for many cryogenic solutions the compression/liquefaction work necessary for the CO₂ transport is minimized.

According to chemical thermodynamics, the minimum work of separation required to separate CO₂ from the other flue gases (inert) involves overcoming the thermodynamic barrier associated to the gas mixing. This corresponds to the opposite of the Gibbs energy of mixing between two products (p_1 , p_2) and the feed (f) in a generic separator, as indicated by Equation (4) [13,42]. In addition, the subsequent compression and/or liquefaction of CO₂ is a crucial aspect in evaluating the efficiency and feasibility of carbon capture processes [13,22]. A more accurate calculation can be attained by including the theoretical work of compression and/or liquefaction to deliver CO₂ in a dense phase. For instance, purified CO₂ must be usually compressed to very high pressures to overcome the pressure drops in the pipelines and to be injected in the form of supercritical fluid into reservoirs at depths of the km order of magnitude. The minimum work required to compress the purified CO₂ is calculated by Equation (5) and corresponds to a reversible isothermal compression. Considering a hydrostatic pressure of roughly 1 MPa per 100 m of depth, the battery limits for CO₂ delivery would be around 10–15 MPa. Alternatively, a liquefaction process can be considered by including the theoretical heat removal by liquefaction in a reversible refrigeration cycle, as reported in Equation (6).

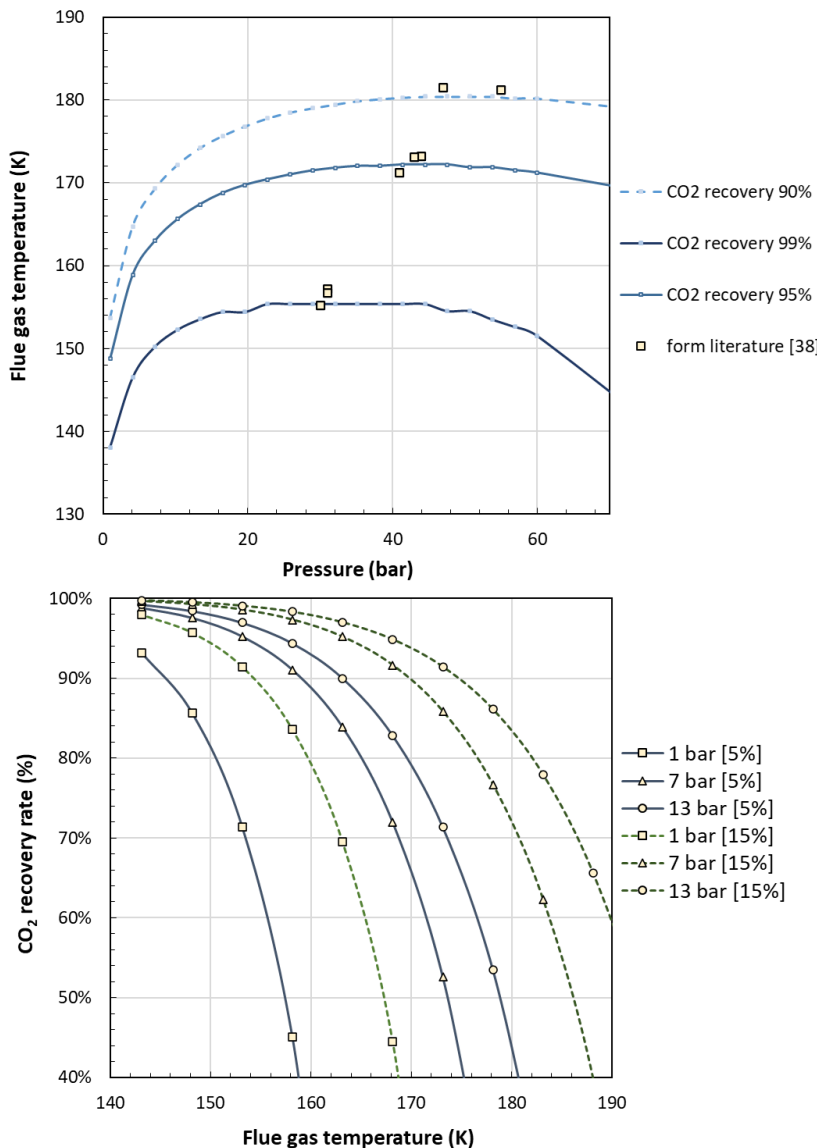


Figure 1. a) SVE calculations of CO₂ recovery in the solid phase as a function of flue gas temperature for different pressures and inlet CO₂ concentrations and b) SVE calculations of flue gas temperature as a function of pressure for different CO₂ recoveries in the solid phase. Simulation results obtained using the RGibbs reactor in Aspen Plus (lines) are compared with data from literature (symbols) [38,40].

In chemical thermodynamics, the minimum work of separation required to separate CO₂ from the other flue gases (inert) involves overcoming the thermodynamic barrier associated to the gas mixing. This corresponds to the opposite of the Gibbs energy of mixing between two products (p_1, p_2) and the feed (f) in a generic separator, as indicated by Equation (4) [13,42]. In addition, the subsequent compression and/or liquefaction of CO₂ is a crucial aspect in evaluating the efficiency and feasibility of carbon capture processes [13,22]. A more accurate calculation can be attained by including the theoretical work of compression and/or liquefaction to deliver CO₂ in a dense phase. For instance, purified CO₂ must be usually compressed to very high pressures to overcome the pressure drops in the pipelines and to be injected in the form of supercritical fluid into reservoirs at depths of the km order of magnitude. The minimum work required to compress the purified CO₂ is calculated by Equation (5) and corresponds to a reversible isothermal compression. Considering a hydrostatic pressure of roughly 1 MPa per 100 m of depth, the battery limits for CO₂ delivery would be around 10–15 MPa. Alternatively, a liquefaction process can be considered by including the theoretical heat removal by liquefaction in a reversible refrigeration cycle, as reported in Equation (6).

$$W_{sep}^{min} = RT[n_c^{CO_2} \ln(y_c^{CO_2}) + n_c^{inert} \ln(n_c^{inert})] + RT[n_b^{CO_2} \ln(y_b^{CO_2}) + n_b^{inert} \ln(n_b^{inert})] - RT[n_m^{CO_2} \ln(y_m^{CO_2}) + n_m^{inert} \ln(n_m^{inert})] \quad (4)$$

$$W_{comp}^{min} = R \cdot T \cdot \ln\left(\frac{P_{out}}{P_{in}}\right) \quad (5)$$

$$W_{cond}^{min} = Q_{cond} \cdot \left(\frac{T}{T_{cond}} - 1\right) \quad (6)$$

$$\eta_{II} = \frac{W_{sep}^{min} + W_{comp}^{min} + W_{cond}^{min}}{W_{sep} + Q_{sep} \cdot \left(1 - \frac{T_0}{T_{sep}}\right) + W_{comp} + W_{cond}} \quad (7)$$

Where the specific thermal duty for condensation Q_{cond} coincides to the latent heat of vaporization. The minimum work of separation is reported in Figure 2 for an inlet CO₂ concentration of 15% as a function of the CO₂ recovery in the solid phase. The calculated value for separating 90% of CO₂ into a pure CO₂ stream and a second N₂-enriched stream is 140 kJ_e kg_{CO₂}⁻¹. By considering a liquefaction occurring at 50 bar, and a work of compression also at 50 bar, the resulting total minimum work of separation is around 400 kJ_e kg_{CO₂}⁻¹. In fact, it has been reported that optimized compression and liquefaction with external refrigeration (e.g., ammonia refrigeration cycle) consume about 100 kWh t_{CO₂}⁻¹ [43]. These values can be compared to the actual work of separation, which can be expressed through the II law efficiency shown in Equation (7). Quantifying the contributions from an energy point of view allows us to use a second law efficiency and therefore to compare a theoretical separation work with the thermal or mechanical energy used in a real system. In fact, the numerator of Equation (7) represents the useful product while the denominator represents the equivalent work including the transformation of thermal energy into mechanical energy (higher quality). More refined methods are presented in the cited literature [13,44,45]. The actual work of separation could then represent a better comparison with the real energy penalties obtained in the CCS projects deployed worldwide.

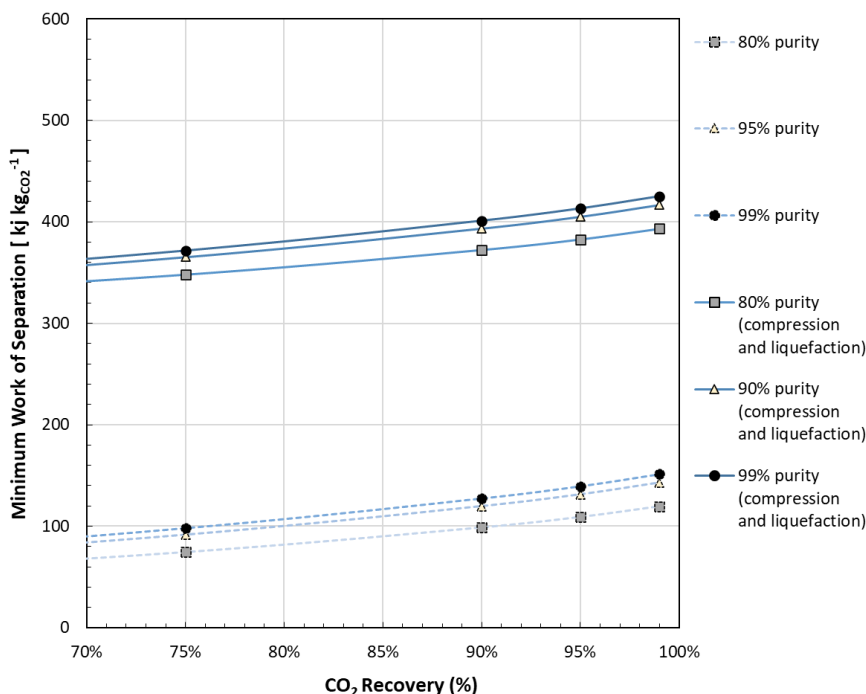


Figure 2. Minimum work of separation to obtain purified CO₂ streams from a 15% CO₂ feed stream as a function of CO₂ recovery in the solid phase. Dotted lines represent the minimum work of separation only. Continuous lines represent the total minimum work of separation including the works of CO₂ compression and liquefaction.

To account for the energy consumption in a cryogenic desublimator we can refer to the schematic shown in Figure 3 adapted from Swanson et al. [22], who performed theoretical calculations for energy penalties associated to CCC. In the figure, the flue gas is pre-cooled by recovering the internal cold energy, including the cold CO_2 product and the cold CO_2 -lean flue gas streams. Recuperative heat exchangers are expected to pre-cool the incoming flue gas. Depending on the operating conditions, the recovery ration and the selected temperature pinch within the recuperative heat exchanger, the process may require an external refrigeration cycle. As can be seen from the figure, there are two types of heat removal strategies: i) cold energy recovery from internal process streams such as the clean gas or the recovered liquid CO_2 ; ii) refrigeration by expending mechanical/electrical energy, i.e. using a refrigeration cycle. According to Swanson et al. [22], and as reported in some real process schemes, two types of refrigeration cycles could be implemented: one with a higher coefficient of performance (COP) rejecting the heat to an internal stream (e.g., the solid CO_2 is used as a low-temperature heat sink for a portion of the heat that must be rejected by the refrigeration system), and another one with a lower COP rejecting the heat at ambient temperature. Rejecting the heat to a cold stream is less costly than the rejecting the heat at ambient temperature. However, the choice of the refrigeration cycle will depend on the equipment design and the dichotomy between capital costs and operational costs due to the low temperatures involved.

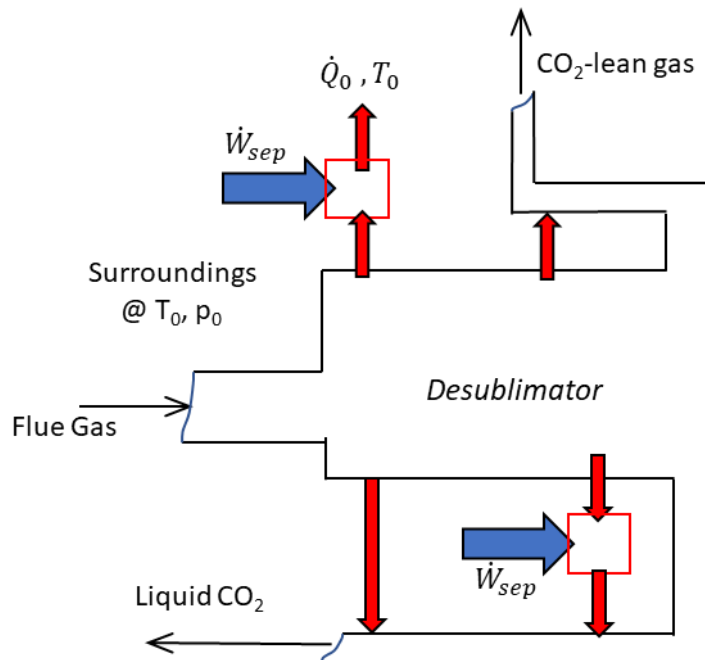


Figure 3. Schematic of a cryogenic desublimator used for theoretical calculations. Adapted from [22].

Downstream of the separation, the energy costs to compress CO_2 to the required pipeline pressures is usually very limited, since CO_2 is already in the liquid phase. For instance, when pressurizing 1 kg of liquid CO_2 at 220 K from atmospheric pressure to 120 bar, the resulting enthalpy change is only 4 kJ. This leads to an overall energy consumption of around $450 \text{ kJ kgCO}_2^{-1}$ with 90% CO_2 recovery, which is comparable to the total minimum works of separation shown in Figure 2. Although the real desublimation processes described in the following sections disclosed slightly higher values of energy consumption, cryogenic processing can be considered very close to the thermodynamic optimum. For instance, in amine-based absorption systems, the energy required for solvent regeneration constitutes a significant portion of the overall work of separation and, if summed to the compression and transportation energy requirements, can total approximately 4–6 MJ kgCO_2^{-1} [13,16]. This means that, compared to the benchmark processes, cryogenic processes can push the II law efficiency of carbon capture from around 20% to more than 50%.

Desublimation can occur from the gaseous bulk phase towards a cold surface or through direct contact with a cold liquid (cryogenic fluid). From the point of view of the design of unit operations, the flue gas can be treated as a stream of non-condensable gases saturated with CO₂ and the formalism presented by classic chemical engineering textbooks can be used to obtain the basic design of the equipment for heat and mass transfer [42]. The heat and mass balances to determine the gas temperature T_G and the gas composition y_{CO_2} along the axial dimension z can be drawn according to the film theory for gas desublimation in a mixture of non-condensable gases in countercurrent contact with a cold liquid, as exhibited in Figure 4. The figure shows the schematics of the film (considering that the liquid cannot vaporize) and the control volumes of the gas flowing from bottom to top and the liquid flowing from top to bottom of a desublimating separator considering 1-dimensional case of a direct-contact desublimating separator. The CO₂ flux occurs through the interface and the separated solid CO₂ fall down into the descending liquid phase that is not volatile (not present in the gaseous phase).

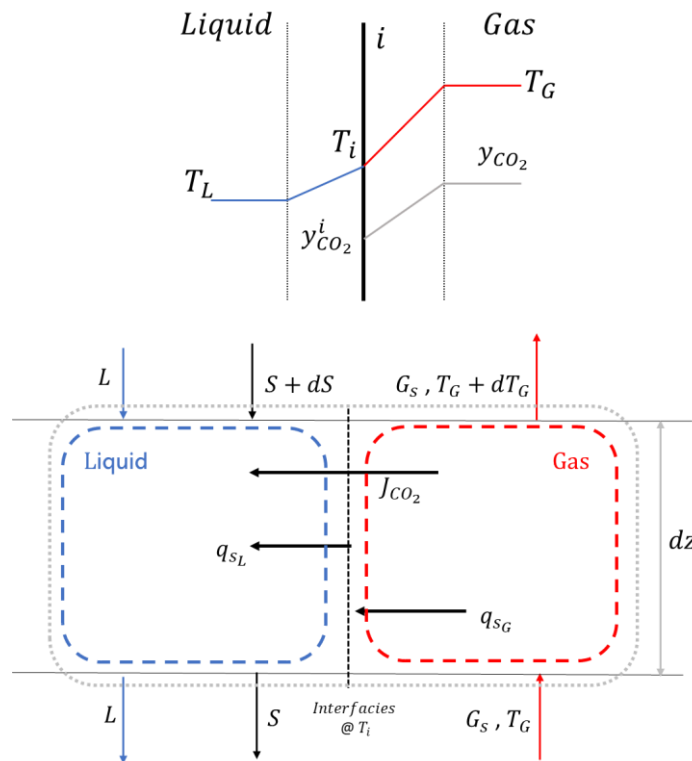


Figure 4. Schematics of the film theory for gas desublimation in a mixture of non-condensable gases in countercurrent contact with a cold liquid.

Heat and mass balances can be generalized by applying them to a control volume between the flue gas mixture from which CO₂ is separated and the cryogenic liquid. Considering a separator section of height dz the following equations represent the heat fluxes exchanged for sensible heat (Equation (8)) and latent heat (Equation (9)) by the gas phase. Equation (10) describe the heat flux transferred to the cryogenic liquid. These equations are also valid for a heat exchanger with a wall between liquid and gas phases under the assumption of the wall having a negligible thermal resistance. By neglecting the sensible heat of solid CO₂ and assuming that the specific surface related to mass transfer coincides with the specific surface related to heat transfer, the balance of fluxes $q_{sL} = q_{sG} + q_{\lambda G}$ can be used to calculate the interface temperature.

$$q_{sG} = h_G \cdot (T_G - T_i) \quad (8)$$

$$q_{\lambda G} = \lambda_{CO_2} \cdot k_Y \cdot (y_{CO_2} - y_{CO_2,i}) \quad (9)$$

$$q_{sL} = h_L(T_i - T_L) \quad (10)$$

The mathematical modelling and the related algorithms to define the temperature – concentration profile of a desublimator are similar to those determined for vapor mixtures containing both condensable and non-condensable gases. Simplified methodologies to calculate the direct contact heat and mass transfer apparatus can be found for systems characterized by a Lewis number approximately equal to 1 (air-water humidification and dehumidification systems) [42]. In this case (CO₂-flue gases-cryogenic liquid), the heat and material balances should be numerically integrated to determine the temperature of the phase interface as well as the temperatures of the liquid and gas phases as well as the CO₂ concentration profile. In the field of desublimation there are no complete theoretical works combining thermodynamic aspects and heat and mass transfer phenomena. A few modelling works are available for desublimation equipment although most of these works have not been fully validated against experimental data. Only Asgharian et al. [32] provided a detailed numerical framework for the modelling of the main components constituting a cryogenic carbon capture process, including CO₂ separators, storage tanks, heat exchangers and turbomachinery. Table 1 details the main modelling features of literature works related to CCC by desublimation.

Table 1. Main modelling features of literature works on cryogenic carbon capture by desublimation.

Reference	Main content and findings
Asgarian et al. [32]	They reviewed thermodynamic framework, general models and process simulator works for calculating equipment for cryogenic process and apparatus. They also included heat exchanger modelling, particle velocity model for heat transfer from or to droplets, plug flow reactor modelling, and Aspen Plus simulations for modelling the LNG storage.
De Guido et al. [35], Pellegrini et al. [38]	They implemented SRK and PR EoS to calculate solid CO ₂ solubilities and proposed a mathematical algorithm developed for the calculation of Solid Vapor Equilibrium stages and compared their results to Aspen RGibbs reactor.
Yu et al. [46]	Numerical analysis of a 1-dimensional desublimating heat exchanger. They calculated the rate of desublimation and thickness of solid formation on the walls as a function of time and location. Both the inert gas (in the gaseous mixture with CO ₂) and the cryogenic liquid are nitrogen. They analysed the effect of fluid mass flow rates and temperatures; they neglected the thermal resistance of the solid CO ₂ layer and pressure drops.
Berger et al. [47]	They proposed a conceptual framework to address the work of separation through cryogenic desublimation; they defined the methodologies for energy balances and energy penalties calculation and proposed the comparison to the minimum work of separation.
Cann [48]	The frost front velocity experiments in a fixed packed bed allowed the design of a moving packed bed (setting the bed flowrate to match the frost front velocity) to prevent the excessive accumulation of CO ₂ frost. He reported heat transfer coefficients, pressure drops and other fundamental correlations to describe experimental data of desublimation in a moving bed.
James [49]	He proposed model predicted the behaviour of a falling sphere heat exchanger in a desublimating columns for CO ₂ capture. Desublimation and condensation of molecules in flue gas streams occurring in a countercurrent falling sphere heat exchanger has been modelled and partially validated with experiments. The model is interesting for spray-chambers but is limited by the fact that the majority of the properties used to calculate heat transfer are at film temperature.
Sun et al. [50], Wu et al. [51], Wu and Webb [52]	Frost formation and frost release on surfaces, frost growth and densification, frost release: modelling experimental results.

Lei et al. [53] CO₂ desublimation on a cooled cylinder surface by means of lattice Boltzmann model with 2D simulations, various behaviours in response to different operation conditions.

3. Processes Based on Cryogenic Desublimation

Cryogenic carbon capture based on SVE takes advantage of the unique thermodynamic property that CO₂ exists in gaseous phase at atmospheric pressure, and, therefore, desublimates to a solid phase in a temperature range of 130–180 K, depending on its concentration in the flue gases. This is because CO₂ exhibits an exceptionally high triple point pressure of 518 kPa [54]. This separation method can obtain very high CO₂ purities (99.9%) and CO₂ recoveries (90–99%) simultaneously, along with ease of CO₂ transportation and storage. However, as already mentioned, there also exist important limitations associated to this technology including the risk of blockages from condensed water, CO₂ frosting in pipelines and storage tanks, and increased capture costs due the cold energy sources [31,55].

Nevertheless, for post-combustion carbon capture applications, i.e., when the CO₂ concentration in the flue gases ranges 5–15 mol%, cryogenic desublimation has shown a substantial lower energy consumption compared to other technologies, even in the cryogenic sector, e.g., cryogenic distillation and condensation. Being based on liquid-vapor equilibrium, in fact, cryogenic distillation requires higher operational pressures and has been successfully proposed for treating gas mixtures with a high CO₂ content (20–70 mol%), such as natural gas, shifted syngas and biogas streams [23,26].

The block flow diagram of a generic cryogenic desublimation process is shown in Figure 5. The flue gases are first dried to remove the moisture content and then cooled down below the freezing temperature of CO₂, where the gas desublimates at a temperature range defined by the CO₂ concentration in the flue gases and the capture efficiency of the process. Solid CO₂ is then separated and normally liquefied for ease of transportation and storage. Several process configurations feature additional steps of pre-treatment, compression, expansion as well as heat integration in-between the main steps of Figure 5. In the next sub-sections the latest developments and challenges of the post-combustion carbon capture processes based on cryogenic desublimation will be presented and discussed.

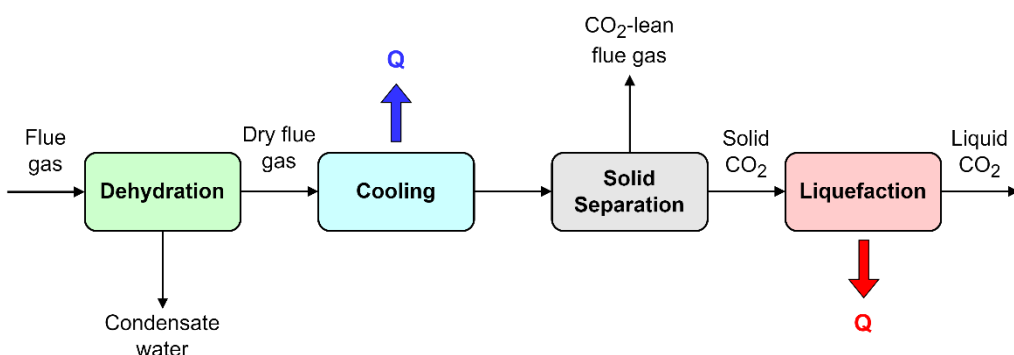


Figure 5. Block flow diagram of a generic cryogenic desublimation process.

3.1. Dynamic Packed Bed

The concept of using cryogenic packed beds operated cyclically to capture CO₂ from flue gases was first introduced by Tuinier et al. [29]. According to this method, CO₂, H₂O and atmospheric gases (N₂, O₂, Ar) can be effectively separated on the basis of the differences in their dew and sublimation points. Furthermore, disadvantages related to frost clogging, high pressure drops, the use of chemical sorbents and elevated operational pressures can all be avoided. To allow a continuous separation, Tuinier et al. [56] designed a 3-bed, 3-step cycle configuration consisting of a cooling, a capture and a recovery step, similarly to a conventional cyclic adsorption-based process [57]. In the cooling step, the bed is cryogenically cooled down to -120°C with the aid of cold energy provided by the

vaporization of LNG. In the capture step, the feed gas is passed through the bed where H_2O and CO_2 condensate and sublimate, respectively, on the bed packing while supercritical N_2 leaves the bed outlet. Then, in the recovery step, CO_2 and H_2O are recovered via a co-current purging stream of pure CO_2 and air, respectively. The process flow diagram of the cryogenic packed bed is reported in Figure 6. The same authors [29,56] studied the evolution of concentration and temperature profiles along the bed axial dimension by experiments and dynamic simulations using a 1D pseudo-homogeneous model. It was found that starting from a flue gas containing 10 mol% CO_2 and 1 mol% H_2O (balanced with N_2) at atmospheric pressure, the required cold duty to carry out the separation was $1.8 \text{ MJ kg}_{\text{CO}_2}^{-1}$. In a follow up work, Tuinier et al. [58] performed a techno-economic assessment of the cryogenic packed bed-based technology. The influence of several parameters was investigated including the initial bed temperature, the feed CO_2 concentration as well as the resulting pressure drops. Compared to other carbon capture methods, this technology was found to experience greater heat losses and to heavily rely on the availability of the cold utilities. In the above works the employed packing material was a steel monolith structure, however, Lively et al. [59] proposed to use fibrous packing in order to increase the contact area and reduce the purging gas pressure drops along the bed. It was claimed that these fibrous materials have the potential to foster the scale-up of this technology from both capital and operational cost perspectives.

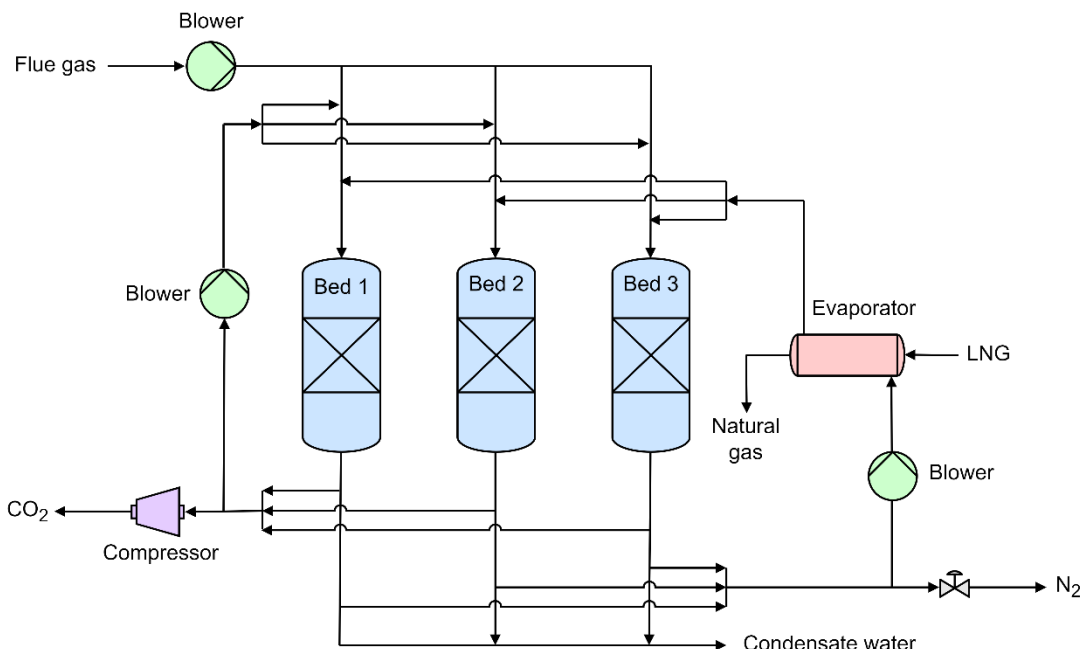


Figure 6. Process flow diagram of the cryogenic packed bed technology [58].

A major limitation of this technology is that the process output is a gaseous stream of CO_2 that must be returned to the liquid phase for transportation and storage, therefore losing the advantage of avoiding the liquefaction cost. Other limitations in the use of fixed packed beds are that the CO_2 frost can accumulate in the bed during the capture step, thus hindering the heat transfer efficiency, and the need of multiple beds to be operated cyclically. To overcome these issues, Willson et al. [60] introduced the moving packed bed technology where the CO_2 frost is removed more efficiently from the capture bed and is recirculated for pre-cooling purposes. The process was modelled using Aspen Plus software for flue gases having a CO_2 concentration in the range of 5–35 mol%. The cryogenic moving bed technology showed significantly lower CO_2 capture costs than the conventional amine-based absorption process for small-scale applications. In subsequent works, Cann et al. [61,62] conducted experimental works to assess the behaviour of temperature profiles within the moving packed beds. The key findings were: i) the CO_2 frost accumulation front can be controlled in the capture bed under appropriate conditions; ii) high-density ceramic packing allowed higher front velocities than steel-based packing; iii) bed pre-cooling and CO_2 capture steps can be operated

simultaneously. In addition, the design of cryogenic moving beds could be optimized by incorporated appropriate energy balance models involving CO₂ desublimation for various gas feed flowrates and compositions, as recently investigated by Cann and Font-Palma [63].

3.2. External Cooling Loop

Since 2008 Sustainable Energy Solutions have developed a cryogenic carbon capture process based on a minimally invasive bolt-on technology for post-combustion able to reuse waste cold energy by an external cooling loop [64]. This method features additional benefits such as reduced compression power, water savings and simultaneous treatment of pollutants (SO_x, NO_x, HCl). In the original process configuration [40], the flue gas is initially dried and cooled to a temperature just above the CO₂ freezing point through an external refrigerant loop. The CO₂ is then expanded for further cooling and desublimated in a gas-solid separator. The solid CO₂ is eventually liquefied by exchanging heat with the incoming feed. However, the process was improved by Jensen et al. [30], as reported in Figure 7. After drying, the flue gas enters a multi-stream heat exchanger where its temperature is lowered to -98°C. The flue gas is then further cooled to -119°C in a staged column with direct cryogenic liquid contact, causing CO₂ to desublimate. The resulting slurry of solid CO₂ and contacting liquid is sent to a separator after which the dry ice is melted in the multi-stream heat exchanger providing liquid CO₂. The melting heat exchanger is also integrated to recover the cold thermal duty. On the other side, the contacting liquid stream is cooled by an LNG-based external refrigeration loop and sent back to the staged column. According to the authors' simulation results (Jensen et al. [30]), this technology could recover 90% of CO₂ with an energy consumption of 0.74 MJ_e kg⁻¹ CO₂ when retrofitted to a 550 MW_e coal-fired power plant. In addition, a recent patent [65] disclosed an invention to further improve the energy efficiency of the process by using multiple external cooling loops and matching the temperature profiles between the condensable vapor and the refrigerant, up to temperature differences of less than 1°C. It was also reported [66] that the external cooling loop technology has the capability of storing energy in the form of LNG, allowing to shift the parasitic losses during peak hours and regenerating the refrigerant during low-demand periods. The cryogenic carbon capture process could thus be optimized within a hybrid energy system coupling both conventional and renewable power generation units.

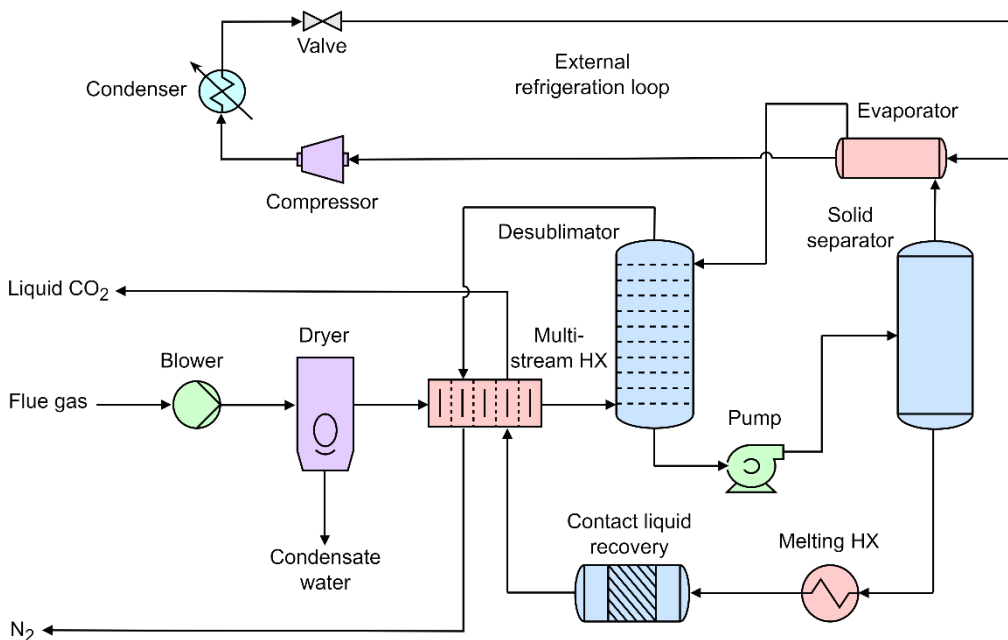


Figure 7. Process flow diagram of the external cooling loop technology [30].

A strong advantage of the external cooling loop technology is that it has been successfully tested on real flue gas slip streams from coal, biomass, natural gas and municipal waste fuels at various field sites in Utah and Wyoming, USA, including utility power stations, heating plants and cement kilns [64]. The CO₂ concentration in the feed ranged 5–22 mol% on dry basis while the CO₂ recoveries were between 90 and 99%. In a recent technical report by Sustainable Energy Solutions [67], it was claimed that multiple tests using the flue gas at the Hunter power plant exceeding 35 hours were completed, with a total of over 600 hours of CO₂ capture with an average CO₂ recovery of over 91%.

3.3. Stirling Cooler

Free piston Stirling coolers are a new type of cryogenic coolers that are attracting interest due to their high energy efficiency and operation reliability. Differently from conventional coolers, they could be regenerated using helium or hydrogen as working fluids, thus avoiding the use of environmentally harmful gases such as CFCs and HCFCs [68]. Because of these advantages, Song et al. [69] proposed to incorporate the Stirling coolers within the cryogenic post-combustion capture process. The process flow diagram coupled with heat integration is shown in Figure 8. The system is composed of three sections, namely pre-freezing tower, main freezing tower and storage tower, each of them being refrigerated by a Stirling cooler. The flue gas is compressed and, after recovering heat from the outgoing process streams, is sent to the pre-freezing tower where the temperature is controlled by the first Stirling cooler. In this tower water is removed from the flue gas by condensation. The dry flue gas is then passed through the main freezing tower where additional heat is removed by the second Stirling cooler until the temperature reaches -140°C. At which point CO₂ desublimates and the solid dry ice is scraped down by a rod to gather on the storage tower (refrigerated by the third Stirling cooler). Eventually, the CO₂-lean flue gas leaves the top of the main freezing tower while the captured CO₂ is collected at the bottom of the storage tower (Figure 8).

The cryogenic CO₂ capture process based on free piston Stirling coolers has been extensively assessed both numerically and experimentally. In particular, Song et al. [70] carried out a detailed parametric analysis on a mathematical model coupling mass and energy balances. They investigated the influence of various parameters on the CO₂ capture rate and the energy consumption, including the ambient temperature, the vacuum condition on the interlayer, the idle operating time, the flue gas flowrate as well as the Stirling cooler temperatures. The system was further optimized using a surface response methodology on the basis of experimental data fitting to a second-order polynomial and an analysis of variance (ANOVA). It was found that the optimal process could achieve 95% of CO₂ capture rate with a specific energy consumption of 0.55 MJ_e kg_{CO2}⁻¹ [71]. These results were also fully confirmed experimentally using a lab-scale apparatus considering a reference flue gas flowrate of 5 L min⁻¹ at atmospheric pressure [72]. In order to enhance the cryogenic CO₂ capture efficiency, Song et al. [68] studied the coefficient of performance (COP) of the Stirling coolers in a follow up experimental work. According to the key findings, the COP could be increased up to a value of 0.82 by designing short and thick cold heads and using copper as a material of construction. More recently, an advanced cryogenic CO₂ capture process based on Stirling coolers was also simulated and optimized by heat integration using Aspen Plus software. It was concluded that only two Stirling coolers would be required in the system while the energy consumption could be reduced by 45.1%, when applying the process to the flue gas of a conventional 600 MW coal-fired power plant [73].

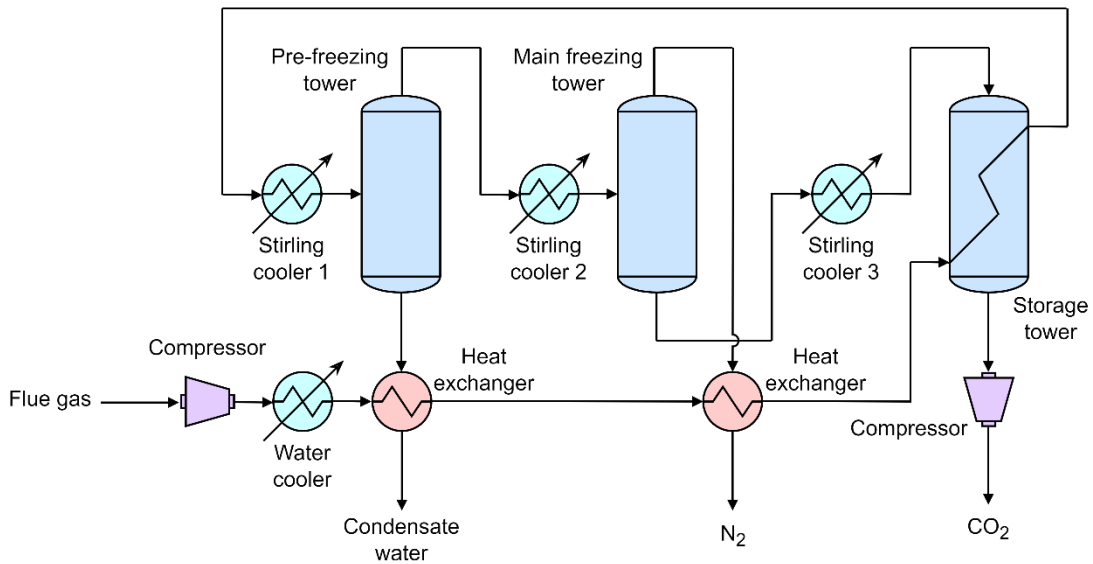


Figure 8. Process flow diagram of the Stirling cooler technology [73].

3.4. Antisublimation (AnSU)

The first cryogenic process based on desublimation was developed by Clodic and Younes [74], who aimed to capture CO₂ by freezing it on the cold surfaces of low-temperature evaporators. The authors proposed a thermodynamic cycle considering the variation of CO₂ freezing temperature at atmospheric pressure as a function of the CO₂ concentration in the feed. For instance, with initial concentrations of 15 mol% and 1 mol%, the freezing temperatures are around -100°C and -122°C, respectively [75]. The patented process was called Antisublimation (AnSU) [76] and consisted of five steps, as presented in Figure 9. The flue gas is first sent to three condensers in series where it is ultimately cooled down to -40°C for water removal. On the other side the CO₂-lean flue gas is recirculated through three evaporators in series designed for heat integration. Further heat is also recovered in the pre-cooler where the dry flue gas temperature is lowered to -100°C by exchanging heat with the cold CO₂-lean flue gas. An LNG-based refrigeration integrated cascade (RIC) equipped with a single compressor and integrated with the water cooling loop provides to the cold energy duty to the desublimation unit through the evaporation of the refrigerant blend occurring between -120°C and -100°C. In the desublimator CO₂ is captured as dry ice with a temperature glide corresponding to the decrease of CO₂ concentration in the flue gas associated to the capture process. A CO₂ recovery system inside the desublimator allows to recover the heat of fusion and some heat of sublimation of CO₂ so that both liquid CO₂ and gaseous CO₂ are produced and collected in a downstream tank (Figure 9).

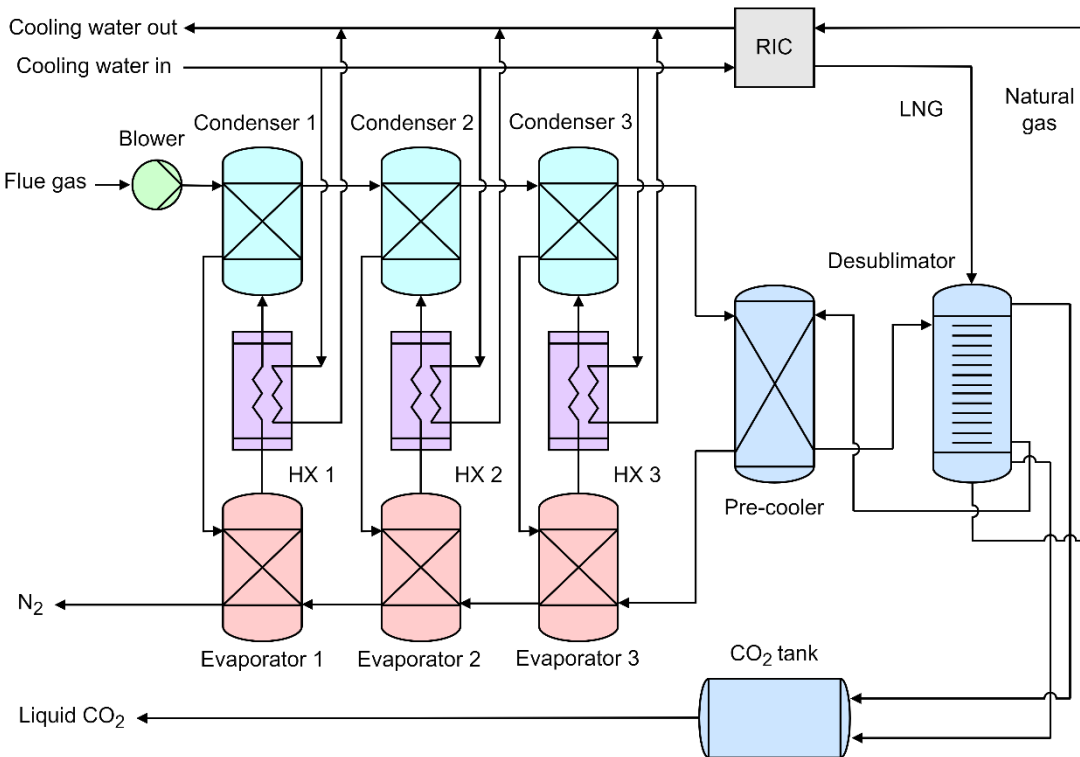


Figure 9. Process flow diagram of the AnSU technology [54].

The AnSU process was extensively assessed both theoretically and experimentally. Clodic et al. [77] studied the COP of the RIC of a post-combustion CO₂ capture process applied to a pulverized coal-fired power plant. It was found that with an initial CO₂ concentration of 10% in the feed and a CO₂ recovery of 90%, the specific energy consumption ranged between 0.65 and 1.25 MJ_e kgCO₂⁻¹ depending on the cooling system efficiency. Pan et al. [54] improved the calculations concerning the energy penalty incurred by a 900 MW coal-fired power plant considering all electrical equipment along with the CO₂ compression power. The resulting energy consumption associated to the anti-sublimation process was 1.18 MJ_e kgCO₂⁻¹ for a CO₂ initial concentration of 12% and a CO₂ capture rate of 90%. These theoretical results were also confirmed by experimental tests on a mock-up of 2.5 kW cooling capacity at -120°C running for 4000 hours and capturing 150 kg of CO₂ per day [54,75]. Due to the cryogenic temperature range of operation of the AnSU process, even a slight increase in the temperature of the cold refrigerant may result in a significant reduction in the overall energy consumption of the system. For this reason, Hees and Monroe [78] have disclosed the idea of carrying out the desublimation step at a higher pressure than atmospheric pressure, in the range of 1.5–10 bar. It was claimed that this would allow an increase of the refrigerant temperature, while still retaining the CO₂ capture efficiency.

3.5. Novel Low-Cost CO₂ Capture Technology (NLCCT)

De and Oduniyi [79] recently disclosed a cryogenic CO₂ post-combustion capture technology, called NLCCT, characterized by low cost and low water consumption. This method features the simultaneous removal of all typical flue gas pollutants (SO_x, NO_x, HCl, CO, Hg, ashes, etc.), the use of cold nitrogen gas as refrigerant, the use of turbine expansion work to drive some of the compressor shafts and some efficiently constructed cooling chambers to pre-cool and desublimate CO₂. The process flow diagram of the NLCCT technology is exhibited in Figure 10. The cold N₂ gas is produced in a refrigeration cycle where N₂ at ambient conditions is first sent to a 5-stage intercooled compressor to raise its pressure to 25–40 atm. After being cooled down to 37°C in a condenser, the N₂ is then expanded in a turbo-expander to 1 atm where it cools down to the desired temperature range of -175/-102°C. This cold N₂ stream along with the recirculated CO₂-lean flue gas will provide the cold

duties to the water condenser, the pre-coolers and the desublimator, as illustrated in Figure 10. On the other side, the flue gas is first passed through a water condenser allowing the removal of H_2O , and then is directed to two pre-coolers where its temperature is lowered just above the CO_2 freezing point, thus preventing premature CO_2 desublimation that could cause fouling. Eventually, upon further cooling, CO_2 is recovered in the solid state at the bottom of the desublimation chamber while the CO_2 -lean flue gas leaves at the top of the chamber.

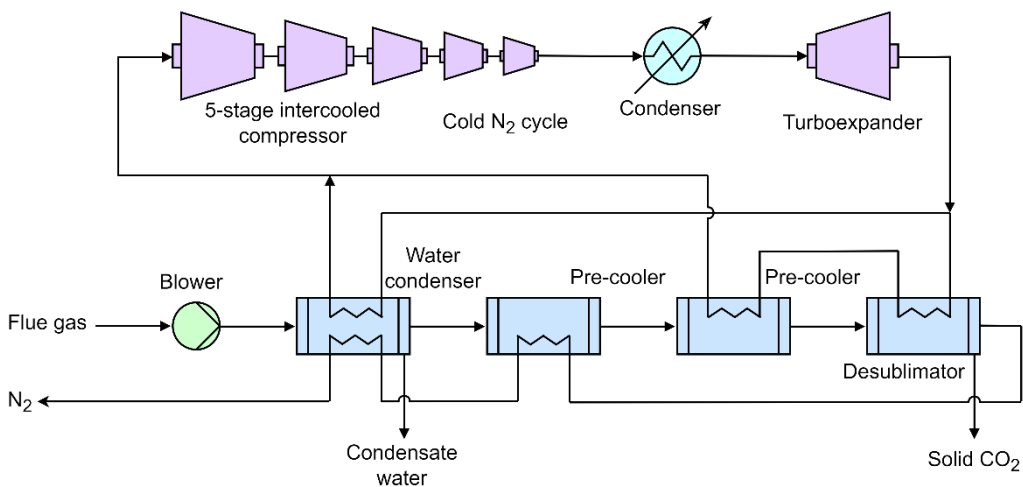


Figure 10. Process flow diagram of the NLCCT technology [80].

De et al. [80] performed an in-depth modelling assessment of the NLCCT process applied to natural gas-fired combined cycle power plants, evaluating several parameters such as CO_2 concentration in the feed, ambient temperature, compression temperatures and pressure ratios. With a CO_2 concentration in the feed of 6.7 mol%, the system achieved a CO_2 capture efficiency of 99% along with a specific energy consumption of 0.63 $\text{MJ}_e \text{ kg}_{\text{CO}_2}^{-1}$.

3.6. Comparison of Cryogenic Desublimation Processes

The main advantages and challenges of the cryogenic processes by desublimation for post-combustion carbon capture described in the previous sub-sections are reported in Table 2. It is clear from the table that apart from the AnSU process all technologies can treat wet flue gases, some of them even showing the capability of removing other pollutants. In addition, the external cooling loop, the Stirling cooler and the NLCCT process feature energy storage and/or water saving potentials. At the same time, only the external cooling loop and the AnSU process have been tested on a pilot plant scale, while the other technologies are only limited to lab-scale demonstrations and/or numerical studies. Because of the high energy requirements of cryogenic processes, their installation is usually restricted by the availability of cold energy sources, especially LNG for dynamic packed bed and AnSU, which, in turn, are subject to the scale, location and other specifications of the natural gas plants. Although less cost-effective, compression and refrigeration are a common method to provide the cold energy duties, to be ideally integrated with recuperative heat exchangers to recover sensible and latent heats from residual streams and the liquefaction of solid CO_2 (Stirling cooler, NLCCT). Furthermore, most technologies suffer from heat losses due to CO_2 frost accumulation during the desublimation [31].

Table 2. Advantages and challenges of cryogenic CO₂ capture processes based on desublimation.

Cryogenic process	Advantages	Challenges
Dynamic packed bed	<ul style="list-style-type: none"> • Operating at atmospheric pressure • Low pressure drops • Simultaneous removal of H₂O and CO₂ 	<ul style="list-style-type: none"> • Relying on availability of LNG • Heat losses due to CO₂ frost accumulation in packed beds
External cooling loop	<ul style="list-style-type: none"> • Relatively high TRL • Energy storage potential • Simultaneous treatment of pollutants • Operating at atmospheric pressure 	<ul style="list-style-type: none"> • High capital cost • Need of multiple and/or mixed refrigerants
Stirling cooler	<ul style="list-style-type: none"> • Energy storage potential • Simultaneous removal of H₂O and CO₂ • Relatively high TRL 	<ul style="list-style-type: none"> • Heat losses due to CO₂ frost accumulation in heat exchangers • System oscillations
AnSU	<ul style="list-style-type: none"> • Recovery of CO₂ latent heat of fusion • Low operational cost 	<ul style="list-style-type: none"> • Relying on availability of LNG • Heat losses due to CO₂ frost accumulation in heat exchangers
NLCCT	<ul style="list-style-type: none"> • Water savings potential • Simultaneous treatment of pollutants 	<ul style="list-style-type: none"> • Low heat transfer rates of cold N₂ gas • No experimental campaign

Table 3 summarizes the separation performances of the cryogenic CO₂ capture processes by desublimation. Although the processes cannot be directly compared due to the different CO₂ concentrations in the feed and the CO₂ recoveries achieved, the Stirling cooler and the NLCCT process seem more promising, with specific energy consumptions in the range of 0.55–0.63 MJ_e kg_{CO₂}⁻¹¹. However, the results from the external cooling loop and AnSU technologies should provide once again a better indication of the energy consumption figures (0.74–1.18 MJ_e kg_{CO₂}⁻¹) as they were tested on a pilot plant scale. It should be noted that all cryogenic processes in Table 3 have been compared based on electrical energy consumption, where the conversion ratio between thermal and electrical energy is around 0.5 for this kind of applications [56].

Table 3. Performance comparison of cryogenic CO₂ capture processes based on desublimation.

Cryogenic process	Feed CO ₂ concentration (mol%)	Cold energy source	CO ₂ recovery (%)	Minimum specific energy consumption (MJ _e kg _{CO₂} ⁻¹)	Type of study	Reference
Dynamic packed bed	10	LNG	99	3.60	Experimental & Modelling	Tuinier et al. [56]
External cooling loop	16	Multiple refrigerants	90	0.74	Experimental & Modelling	Jensen et al. [30]
Stirling cooler	13	Stirling cooler	95	0.55	Experimental & Modelling	Song et al. [71]
AnSU	12	LNG	90	1.18	Experimental	Pan et al. [54]
NLCCT	6.7	Cold N ₂ gas	99	0.63	Modelling	De et al. [80]

4. Conclusions and Future Directions

Cryogenic carbon capture by desublimation has emerged in the last two decades as a promising carbon capture technology due to the understanding of fundamental thermodynamic aspects and mass transfer phenomena along with strong advances in the process configurations aimed to maximize the energy recovery and decrease the overall costs. In particular, the external cooling loop and AnSU technologies have been tested on pilot plant level and reported energy consumptions in the range of 0.74–1.18 MJ_e kg_{CO₂}⁻¹. In addition, detailed modelling works based on the Stirling cooler and NLCCT process claimed even lower energy consumptions and thus overall costs.

At the same time several knowledge gaps and research needs have to be addressed in order to achieve a practical implementation of CCC. Key research areas are as follows:

- The operating conditions of CCC, including temperature ranges, pressure levels, and heat integration potential need to be further optimized. Understanding the influence of these process variables on the separation efficiency as well as the energy consumption is pivotal for scale-up and commercialization purposes.
- Assessing the economic viability of CCC and identifying strategies to reduce costs are critical knowledge gaps. Research should focus on the development of cost-effective materials and innovative engineering solutions at cryogenic conditions to enhance the overall economic feasibility. This should include insulation materials, equipment materials, and additional materials for constructing heat exchangers.
- Understanding how CCC can be effectively integrated into various industrial processes is another key research aspect. This encompasses the retrofit of CCC with various industries, identifying potential synergies and addressing engineering challenges.
- Investigating the safety aspects and potential risks associated with CCC is paramount. Research needs to be carried out on the behavior of cryogenic fluids, their associated hazards and the development of robust safety protocols to ensure the protection of personnel and the environment.
- A comprehensive assessment of the environmental impact of CCC is necessary. This should involve evaluating the overall carbon footprint of the technology, including indirect emissions associated with equipment production, transportation, and other life cycle stages.

Author Contributions: Conceptualization, M.C. and M.L.; methodology, M.C. and M.L.; data curation, M.C., E.B. and M.L.; writing—original draft preparation, M.C., E.B. and M.L.; writing—review and editing, M.C., E.B. and M.L. All authors have read and agreed to the published version of the manuscript.

Funding: This research received no external funding.

Data Availability Statement: No new data were created or analyzed in this study. Data sharing is not applicable to this article.

Conflicts of Interest: The authors declare no conflicts of interest.

Nomenclature

Acronyms

AnSU	Antisublimation
BECCS	Bioenergy with carbon capture and storage
CCC	Cryogenic carbon capture
CCS	Carbon capture and storage
CCU	Carbon capture and utilization
CCUS	Carbon capture, utilization and storage
COP	Coefficient of performance
DAC	Direct air capture
EoS	Equation of state
NLCCT	Novel low-cost CO ₂ capture technology
PSA	Pressure swing adsorption
RIC	Refrigeration integrated cascade

Symbols	Unit	Description
SMR		Steam methane reforming
SVE		Solid-vapor equilibrium
SLVE		Solid-liquid-vapor equilibrium
TRL		Technology readiness level
TSA		Temperature swing adsorption
<i>a</i> (<i>T</i>)	Pa m ⁶ mol ⁻²	Energy parameter in cubic EoS
<i>b</i>	m ³ mol ⁻¹	Covolume in cubic EoS
<i>h_G</i>	W m ⁻² K ⁻¹	Heat transfer coefficient of the gas phase
<i>h_L</i>	W m ⁻² K ⁻¹	Heat transfer coefficient of the liquid phase
<i>k_Y</i>	kg m ⁻² s ⁻¹	Mass transfer coefficient of the gas phase
<i>n_f^{CO₂}</i>	mol	Moles of CO ₂ in the feed
<i>n_{p1}^{CO₂}</i>	mol	Moles of CO ₂ in the product 1
<i>n_{p2}^{CO₂}</i>	mol	Moles of CO ₂ in the product 2
<i>n_f^{inert}</i>	mol	Moles of inert in the feed
<i>n_{p1}^{inert}</i>	mol	Moles of inert in the product 1
<i>n_{p2}^{inert}</i>	mol	Moles of inert in the product 2
<i>P</i>	Pa	Total pressure
<i>P_{CO₂}^S</i>	Pa	Sublimation vapor pressure of CO ₂
<i>P_{in}</i>	Pa	Initial pressure of compression
<i>P_{out}</i>	Pa	Final pressure of compression
<i>Q_{cond}</i>	W	Thermal duty of condensation
<i>Q_{sep}</i>	kJ kg ⁻¹	Specific thermal duty of separation
<i>q_{sG}</i>	W m ⁻²	Sensible heat flux of the gas phase
<i>q_{λG}</i>	W m ⁻²	Latent heat flux of the gas phase
<i>q_{sL}</i>	W m ⁻²	Sensible heat flux of the liquid phase
<i>R</i>	J mol ⁻¹ K ⁻¹	Ideal gas constant
<i>S</i>	m ²	Interface surface
<i>T</i>	K	Temperature
<i>T₀</i>	K	Ambient temperature
<i>T_{cond}</i>	K	Temperature of liquefaction
<i>T_G</i>	K	Temperature of the gas phase
<i>T_i</i>	K	Temperature of the interphase
<i>T_L</i>	K	Temperature of the liquid phase
<i>T_{sep}</i>	K	Temperature of the hot source used for separation
<i>v</i>	m ³ mol ⁻¹	Molar volume in cubic EoS
<i>v_{CO₂}^S</i>	m ³ mol ⁻¹	Molar volume of solid CO ₂
<i>W_{comp}^{min}</i>	kJ kgCO ₂ ⁻¹	Minimum work rate of compression
<i>W_{comp}</i>	kJ kgCO ₂ ⁻¹	Actual work of compression
<i>W_{cond}^{min}</i>	kJ kgCO ₂ ⁻¹	Minimum work of liquefaction
<i>W_{cond}</i>	kJ kgCO ₂ ⁻¹	Actual work of liquefaction
<i>W_{sep}^{min}</i>	kJ kgCO ₂ ⁻¹	Minimum work of separation
<i>W_{sep}</i>	kJ kgCO ₂ ⁻¹	Actual work of separation
<i>y_{CO₂}</i>	—	Mole fraction of CO ₂ in the vapor phase
<i>y_{CO₂,i}</i>	—	Mole fraction of CO ₂ in the interface
<i>y_f^{CO₂}</i>	—	Mole fraction of CO ₂ in the feed
<i>y_{p1}^{CO₂}</i>	—	Mole fraction of CO ₂ in the product 1
<i>y_{p2}^{CO₂}</i>	—	Mole fraction of CO ₂ in the product 2
<i>y_f^{inert}</i>	—	Mole fraction of inert in the feed
<i>y_{p1}^{inert}</i>	—	Mole fraction of inert in the product 1
<i>y_{p2}^{inert}</i>	—	Mole fraction of inert in the product 2
<i>z</i>	m	Axial dimension

Greek letters

η_{II}	–	II law efficiency
λ_{CO_2}	$J \text{ kg}^{-1}$	Heat of liquefaction of CO_2
$\phi_{CO_2}^S$	–	Fugacity coefficient of CO_2 at the saturated solid pressure
$\phi_{CO_2}^V$	–	Fugacity coefficient of CO_2 in the vapor phase

References

1. IPCC, 2021: Summary for Policymakers. In: *Climate Change 2021: The Physical Science Basis. Contribution of Working Group I to the Sixth Assessment Report of the Intergovernmental Panel on Climate Change* [Masson-Delmotte, V., P. Zhai, A. Pirani, S.L. Connors, C. Péan, S. Berger, N. Caud, Y. Chen, L. Goldfarb, M.I. Gomis, M. Huang, K. Leitzell, E. Lonnoy, J.B.R. Matthews, T.K. Maycock, T. Waterfield, O. Yelekçi, R. Yu, and B. Zhou (eds.)]. Cambridge University Press, Cambridge, United Kingdom and New York, NY, USA, pp. 3–32.
2. Gabrielli, P.; Gazzani, M.; Mazzotti, M. The role of carbon capture and utilization, carbon capture and storage, and biomass to enable a net-zero- CO_2 emissions chemical industry. *Industrial and Engineering Chemistry Research* **2020**, *59*, 7033–7045.
3. Keyßer, L.T., Lenzen, M. 1.5 °C degrowth scenarios suggest the need for new mitigation pathways. *Nat Commun* **2021** *12*, 2676.
4. Bednar, J., Obersteiner, M., Baklanov, A., Thomson, M., Wagner, F., Geden, O., Allen, M., Hall J.W.A., et al. Operationalizing the net-negative carbon economy. *Nature* **2021**; *596*, 377–383.
5. IEA. Energy Technology Perspectives, **2020**. IEA, Paris <https://www.iea.org/reports/energy-technology-perspectives-2020>, Licence: CC BY 4.0
6. Schmitt, T.; Homsy, S.; Mantripragada, H.; Woods, M.; Hoffman, H.; Shultz, T.; Fout, T.; Hackett, G. Cost and Performance of Retrofitting NGCC Units for Carbon Capture: *U.S. Department of Energy Office of Scientific and Technical Information*, **2023**.
7. Capocelli, M.; Luberti, M.; Inno, S.; D'Antonio, F.; Di Natale, F.; Lancia, A. Post-combustion CO_2 capture by RVPSA in a large-scale steam reforming plant. *Journal of CO_2 Utilization* **2019**, *32*, 53–65.
8. Luberti, M.; Brown, A.; Balsamo, M.; Capocelli, M. Numerical analysis of VPSA technology retrofitted to steam reforming hydrogen plants to capture CO_2 and produce blue H₂. *Energies* **2022**, *15*, 1091.
9. Luberti, M.; Ahn, H. Review of Polybed pressure swing adsorption for hydrogen purification. *International Journal of Hydrogen Energy* **2022**, *47*, 10911–10933.
10. Barba, D.; Brandani, F.; Capocelli, M.; Luberti, M.; Zizza, A. Process analysis of an industrial waste-to-energyplant: Theory and experiments. *Process Safety and Environmental Protection* **2015**, *96*, 61–73.
11. Butnar, I.; Cronin, J.; Pye, S., Review of Carbon Capture Utilisation and Carbon Capture and Storage in future EU decarbonisation scenarios, **2020**. *Final report prepared for The Carbon Capture and Storage Association - UCL Energy Institute*.
12. Koeble, B.S.; van den Broek, M.A.; Faaij, A.P.C.; van Vuuren et al, D.P. Uncertainty in Carbon Capture and Storage (CCS) deployment projections: a cross-model comparison exercise. *Climatic Change* **2014**, *123*, 461–476.
13. Capocelli, M.; De Falco, M. Generalized penalties and standard efficiencies of carbon capture and storage processes. *International Journal of Energy Research* **2022**, *46*, 4808–4824.
14. Sifat, N.S.; Yousef, H. A critical review of CO_2 capture technologies and prospects for clean power generation. *Energies* **2019**, *12*, 4143.
15. Kearns, D.; Liu, H.; Consoli, C., Technology Readiness and Costs of CCS. *Global CCS Institute*, **2021**.
16. Ahn, H.; Luberti, M.; Liu, Z.; Brandani, S. Process simulation of aqueous MEA plants for post-combustion capture from coal-fired power plants. *Energy Procedia* **2013**, *37*, 1523–1531.
17. Erto, A.; Silvestre-Albero, A.; Silvestre-Albero, J.; Rodríguez-Reinoso, F.; Balsamo, M.; Lancia, A.; Montagnaro, F. Carbon-supported ionic liquids as innovative adsorbents for CO_2 separation from synthetic flue-gas. *J Colloid Interface Sci.* **2015**, *15*, 41–50.
18. Luberti, M.; Oreggioni, G.D.; Ahn, H. Design of a rapid vacuum pressure swing adsorption (RVPSA) process for post-combustion CO_2 capture from a biomass-fuelled CHP plant. *Journal of Environmental Chemical Engineering* **2017**, *5*, 3973–3982.
19. Luberti, M.; Ahn, H. Design of an industrial multi-bed (V)PSA unit for argon concentration. *Separation and Purification Technology* **2021**, *261*, 118254.

20. Brunetti, A.; Scura, F.; Barbieri, G.; Drioli, E. Membrane technologies for CO₂ separation. *Journal of Membrane Science* **2010**, *359*, 115–125.
21. Font-Palma, C.; Cann, D.; Udemu, C. Review of cryogenic carbon capture innovations and their potential applications. *Journal of Carbon Research* **2021**, *7*, 58.
22. Swanson, C.E.; Elzey, J.W.; Hershberger, R.E.; Donnelly, R.J.; Pfotenhauer, J. Thermodynamic analysis of low-temperature carbon dioxide and sulfur dioxide capture from coal-burning power plants. *Physical Review E* **2012**, *86*, 016103.
23. S. Holmes and J. M. Ryan, Cryogenic distillative separation of acid gases from methane, US Patent 4,318,723, **1982**.
24. Hart, A.; Gnanendran, N. Cryogenic CO₂ capture in natural gas. *Energy Procedia* **2009**, *1*, 697–706.
25. Yousef, A.M.; El-Maghly, W.M.; Eldrainy, Y.A.; Attia, A. New approach for biogas purification using cryogenic separation and distillation process for CO₂ capture. *Energy* **2018**, *156*, 328–351.
26. Shen, M.; Tong, L.; Yin, S.; Liu, C.; Wang, L.; Feng, W.; Ding, Y. Cryogenic technology progress for CO₂ capture under carbon neutrality goals: A review. *Separation and Purification Technology* **2022**, *299*, 121734.
27. Berstad, D.; Skaugen, G.; Roussanaly, S.; Anantharaman, R.; Nekså, P.; Jordal, K.; Trædal, S.; Gundersen, T. CO₂ capture from IGCC by low-temperature synthesis gas separation. *Energies* **2022**, *15*, 515.
28. Eide, L.I.; Anheden, M.; Lyngfelt, A.; Abanades, C.; Younes, M.; Clodic, D.; Bill, A.A.; Feron, P.H.M.; Rojey, A.; Giroudiere, F. Novel capture processes. *Oil and Gas Science and Technology* **2005**, *60*, 497–508.
29. Tuinier, M.J.; van Sint Annaland, M.; Kramer, G.J.; Kuipers, J.A.M. Cryogenic CO₂ capture using dynamically operated packed beds. *Chemical Engineering Science* **2010**, *65*, 114–119.
30. Jensen, M.J.; Russell, C.S.; Bergeson, D.; Hoeger, C.D.; Frankman, D.J.; Bence, C.S.; Baxter, L.L. Prediction and validation of external cooling loop cryogenic carbon capture (CCC-ECL) for full-scale coal-fired power plant retrofit. *International Journal of Greenhouse Gas Control* **2015**, *45*, 200–212.
31. Song, C.; Liu, Q.; Deng, S.; Li, H.; Kitamura, Y. Cryogenic-based CO₂ capture technologies: State-of-the-art developments and current challenges. *Renewable and Sustainable Energy Reviews* **2019**, *101*, 265–278.
32. Asgharian, H.; Iov, F.; Araya, S.S.; Pedersen, T.H.; Nielsen, M.P.; Baniasadi, E.; Liso, V. A Review on process modeling and simulation of cryogenic carbon capture for post-combustion treatment. *Energies* **2023**, *16*, 1855.
33. Aneesh, A.M.; Sam A.A. A mini-review on cryogenic carbon capture technology by desublimation: theoretical and modeling aspects. *Frontiers in Energy Research* **2023**, *11*, 1167099.
34. Yang, W.; Li, S.; Li, X.; Liang, Y.; Zhang, X. Analysis of a new liquefaction combined with desublimation system for CO₂ separation based on N₂/CO₂ phase equilibrium. *Energies* **2015**, *8*, 9495–9508.
35. De Guido, G.; Langè, S.; Moioli, S.; Pellegrini, L.A. Thermodynamic method for the prediction of solid CO₂ formation from multicomponent mixtures. *Process Safety and Environmental Protection* **2014**, *92*, 70–79.
36. De Guido, G.; Pellegrini, L.A. Phase equilibria analysis in the presence of solid carbon dioxide. *Chemical Engineering Transactions* **2021**, *86*.
37. Wang, J.; Wang, Z.; Sun, B. Improved equation of CO₂ Joule–Thomson coefficient. *Journal of CO₂ Utilization* **2017**, *19*, 296–307.
38. Pellegrini, L.; De Guido, G.; Ingrosso, S. Thermodynamic Framework for Cryogenic Carbon Capture. *Proceedings of the 30th European Symposium on Computer Aided Process Engineering 2020 (ESCAPE30)*, Milano, Italy
39. Jensen, M. Energy Process Enabled by Cryogenic Carbon Capture. Brigham Young University BYU Theses and Dissertations **2015** 5711.
40. Baxter, L.; Baxter, A.; Burt, S. Cryogenic CO₂ capture as a cost-effective CO₂ capture process. *International Pittsburgh Coal Conference*, Pittsburgh, USA, **2009**.
41. Yurata, T.; Lei, H.; Tang, L.; Lu, M.; Patel, J.; Lim, S.; Piumsomboon, P.; Chalermsinsuwan, B.; Li, C. Feasibility and sustainability analyses of carbon dioxide – hydrogen separation via de-sublimation process in comparison with other processes. *International Journal of Hydrogen Energy* **2019**, *44*, 23120–23134.
42. Seader, J.D.; Henley, E. Separation Process Principles, **2006**. John Wiley & Sons. Ing.
43. Zonfrilli, M.; Facchino, M.; Serinelli, R.; Chesti, M.; De Falco, M.; Capocelli, M. Thermodynamic analysis of cold energy recovery from LNG regasification. *Journal of Cleaner Production*, **2023**, *420*, 138443.
44. House, K.Z.; Harvey, C.F.; Aziz, M.J.; Schrag, D.P. The Energy Penalty of Post-Combustion CO₂ Capture & Storage and Its Implications for Retrofitting the U.S. Installed Base. *Energy & Environmental Science* **2009**, *2*, 193.

45. Bejan A. Advanced Engineering Thermodynamics. 4th ed. Hoboken, NJ: John Wiley & Sons, Inc.; 2016.
46. Yu, Z.; Miller, F.; Pfotenhauer, J.M. Numerical modeling and analytical modeling of cryogenic carbon capture in a de-sublimating heat exchanger. *IOP Conf. Series: Materials Science and Engineering* **2017**, *278*, 012032.
47. Berger, A.H.; Hoeger, C.; Baxter, L.; Bhowm, A.S. Evaluation of cryogenic systems for post combustion CO₂ capture. *14th International Conference on Greenhouse Gas Control Technologies, GHGT-14*, Melbourne, Australia, **2018**.
48. Cann, D.G. Experimental exploration of cryogenic CO₂ capture utilising a moving bed Thesis submitted in accordance with the requirements of the University of Chester for the degree of Doctor of Philosophy, **2021**.
49. James, D.W. Failing Drop CO₂ Deposition (Desublimation) Heat Exchanger for the Cryogenic Carbon Capture Process. Theses and Dissertations, **2011**. Brigham Young University
50. Sun, B.; Ghatare, S.; Evans, G.M.; Bhatelia, T.; Utikar, R.P.; Pareek, V.K. Dynamic study of frost formation on cryogenic surface. *International Journal of Heat and Mass Transfer* **2020**, *150*, 119372.
51. Wu, X.; Ma, Q.; Chu, F.; Hu, S. Phase change mass transfer model for frost growth and densification. *International Journal of Heat and Mass Transfer* **2016**, *96*, 11–19.
52. Wu, X.M.; Webb, R.L. Investigation of the possibility of frost release from a cold surface. *Experimental Thermal and Fluid Science* **2001**, *24*, 151–156.
53. Lei T.; Luo, K.H.; Hernández Pérez, F.E.; Wang, G.; Wang, Z.; Cano, J.R.; Im, H.G. Study of CO₂ desublimation during cryogenic carbon capture using the lattice Boltzmann method. *Journal of Fluid Mechanics* **2023**, *964*, A1.
54. Pan, X.; Clodic, D.; Toubassy, J. CO₂ capture by antisublimation process and its technical economic analysis. *Greenhouse Gas Science and Technology* **2013**, *3*, 8–20.
55. Rezaei, S.; Liu, A.; Hovington, P. Emerging technologies in post-combustion carbon dioxide capture & removal. *Catalysis Today* **2023**, *423*, 114286.
56. Tuinier, M.J.; van Sint Annaland, M.; Kuipers, J.A.M. A novel process for cryogenic CO₂ capture using dynamically operated packed beds—An experimental and numerical study. *International Journal of Greenhouse Gas Control* **2011**, *5*, 694–701.
57. Luberti, M. Oxygen recovery from ozone generators by adsorption processes. *Adsorption* **2023**, *29*, 73–86.
58. Tuinier, M.J.; Hamers, H.P.; van Sint Annaland, M. Techno-economic evaluation of cryogenic CO₂ capture—A comparison with absorption and membrane technology. *International Journal of Greenhouse Gas Control* **2011**, *5*, 1559–1565.
59. Lively, R.P.; Koros, W.J.; Johnson, J.R. Enhanced cryogenic CO₂ capture using dynamically operated low-cost fiber beds. *Chemical Engineering Science* **2012**, *71*, 97–103.
60. Willson, P.; Lychnos, G.; Clements, A.; Michailos, S.; Font-Palma, C.; Diego, M.E.; Pourkashanian, M.; Howe, J. Evaluation of the performance and economic viability of a novel low temperature carbon capture process. *International Journal of Greenhouse Gas Control* **2019**, *86*, 1–9.
61. Cann, D.; Font-Palma, C.; Willson, P. Experimental analysis of CO₂ frost front behaviour in moving packed beds for cryogenic CO₂ capture. *International Journal of Greenhouse Gas Control* **2021**, *107*, 103291.
62. Cann, D.; Font-Palma, C.; Willson, P. Moving packed beds for cryogenic CO₂ capture: analysis of packing material and bed precooling. *Carbon Capture Science & Technology* **2021**, *1*, 100017.
63. Cann, D.; Font-Palma, C. Evaluation of mathematical models for CO₂ frost formation in a cryogenic moving bed. *Energies* **2023**, *16*, 2314.
64. Sayre, A.; Frankman, D.; Baxter, A.; Stitt, K. Field testing of cryogenic carbon capture. *Carbon Management Technology Conference*, Houston, USA, **2017**.
65. Baxter, L. Systems and methods for separating condensable vapors from light gases or liquids by recuperative cryogenic process. US Patent No. US 10,724,793 B2 to *Hall Labs LLC*, **2020**.
66. Safdarnejad, S.M.; Hedengren, J.D.; Baxter, L.L. Plant-level dynamic optimization of Cryogenic Carbon Capture with conventional and renewable power sources. *Applied Energy* **2015**, *149*, 354–366.
67. Baxter, L.L.; Baxter, A.; Bever, E.; Burt, S.; Chamberlain, S.; Frankman, D.; Hoeger, C.; Mansfield, E.; Parkinson, D.; Sayre, A.; Stitt, K. Cryogenic Carbon Capture Development. Final Technical Report submitted to *US DoE NETL*, **2019**.
68. Song, C.; Lu, J.; Kitamura, Y. Study on the COP of free piston Stirling cooler (FPSC) in the anti-sublimation CO₂ capture process. *Renewable Energy* **2015**, *74*, 948–954.

69. Song, C.; Kitamura, Y.; Li, S.; Ogasawara, K. Design of a cryogenic CO₂ capture system based on Stirling coolers. *International Journal of Greenhouse Gas Control* **2012**, *7*, 107–114.
70. Song, C.; Kitamura, Y.; Li, S.; Jiang, W. Parametric analysis of a novel cryogenic CO₂ capture system based on Stirling coolers. *Environmental Science and Technology* **2012**, *46*, 12735–12741.
71. Song, C.; Kitamura, Y.; Li, S. Optimization of a novel cryogenic CO₂ capture process by response surface methodology (RSM). *Journal of the Taiwan Institute of Chemical Engineers* **2014**, *45*, 1666–1676.
72. Song, C.; Kitamura, Y.; Li, S.; Lu, J. Deposition CO₂ capture process using a free piston Stirling cooler. *Industrial and Engineering Chemistry Research* **2013**, *52*, 14936–14943.
73. Song, C.; Liu, Q.; Ji, N.; Deng, S.; Zhao, J.; Kitamura, Y. Advanced cryogenic CO₂ capture process based on Stirling coolers by heat integration. *Applied Thermal Engineering* **2017**, *114*, 887–895.
74. Clodic, D.; Younes, M. A new method for CO₂ capture: frosting CO₂ at atmospheric pressure. *Greenhouse Gas Control Technologies* **2003**, *I*.
75. Clodic, D.; El Hitti, R.; Younes, M.; Bill, A.; Casier, F. CO₂ capture by anti-sublimation: Thermo-economic process evaluation. *4th Annual Conference on Carbon Capture & Sequestration*, Alexandria, USA, **2005**.
76. Clodic, D.; Younes, M. Method and system for extracting carbon dioxide by anti-sublimation for storage thereof. US Patent No. 7,073,348 B2 to *Armines*, **2006**.
77. Clodic, D.; Younes, M.; Bill, A. Test results of CO₂ capture by anti-sublimation: Capture efficiency and energy consumption for boiler plants. *Greenhouse Gas Control Technologies* **2005**, *II*.
78. Hees, W.G.; Monroe, C.M. Method and system for extracting carbon dioxide by anti-sublimation at raised pressure. US Patent No. 8,163,070 B2 to *Armines*, **2012**.
79. De, D.K.; Oduniyi, I.A. Highly cost effective technology for capture of industrial emissions without reagent for clean energy and clean environment applications. US Patent No. 10,670,334 B2 to *Sustainable Green Power Industries*, **2020**.
80. De, D.K.; Oduniyi, I.A.; Sam, A.A. A novel cryogenic technology for low-cost carbon capture from NGCC power plants for climate change mitigation. *Thermal Science and Engineering Progress* **2022**, *36*, 101495.

Disclaimer/Publisher's Note: The statements, opinions and data contained in all publications are solely those of the individual author(s) and contributor(s) and not of MDPI and/or the editor(s). MDPI and/or the editor(s) disclaim responsibility for any injury to people or property resulting from any ideas, methods, instructions or products referred to in the content.